Inversion of maize leaf nitrogen using UAV hyperspectral imagery in breeding fields

Qiwen Cheng[1,2†], Bingsun Wu[2†], Huichun Ye[3,4], Yongyi Liang[1,2], Yingpu Che[5], Anting Guo[3,4], Zixuan Wang[1,2], Zhiqiang Tao[1], Wenwei Li[1,2], Jingjing Wang[1*]

(1. *School of Tropical Agriculture and Forestry, Hainan University, Haikou 570228, China*;
2. *Rubber Research Institute, Chinese Academy of Tropical Agricultural Sciences, Haikou 571101, China*;
3. *Key Laboratory of Earth Observation of Hainan Province, Hainan Aerospace Information Research Institute, Sanya 572029, Hainan, China*;
4. *Key Laboratory of Digital Earth Science, Aerospace Information Research Institute, Chinese Academy of Sciences, Beijing 100094, China*;
5. *Institute of Crop Science, Chinese Academy of Agricultural Sciences, Beijing 100081, China*)

Abstract: Nitrogen (N) as a pivotal factor in influencing the growth, development, and yield of maize. Monitoring the N status of maize rapidly and non-destructive and real-time is meaningful in fertilization management of agriculture, based on unmanned aerial vehicle (UAV) remote sensing technology. In this study, the hyperspectral images were acquired by UAV and the leaf nitrogen content (LNC) and leaf nitrogen accumulation (LNA) were measured to estimate the N nutrition status of maize. 24 vegetation indices (VIs) were constructed using hyperspectral images, and four prediction models were used to estimate the LNC and LNA of maize. The models include a single linear regression model, multivariable linear regression (MLR) model, random forest regression (RFR) model, and support vector regression (SVR) model. Moreover, the model with the highest prediction accuracy was applied to invert the LNC and LNA of maize in breeding fields. The results of the single linear regression model with 24 VIs showed that normalized difference chlorophyll (NDchl) had the highest prediction accuracy for LNC (R^2, RMSE, and RE were 0.72, 0.21, and 12.19%, respectively) and LNA (R^2, RMSE, and RE were 0.77, 0.26, and 14.34%, respectively). And then, 24 VIs were divided into 13 important VIs and 11 unimportant VIs. Three prediction models for LNC and LNA were constructed using 13 important VIs, and the results showed that RFR and SVR models significantly enhanced the prediction accuracy of LNC and LNA compared to the multivariable linear regression model, in which RFR model had the highest prediction accuracy for the validation dataset of LNC (R^2, RMSE, and RE were 0.78, 0.16, and 8.83%, respectively) and LNA (R^2, RMSE, and RE were 0.85, 0.19, and 9.88%, respectively). This study provides a theoretical basis for N diagnosis and precise management of crop production based on hyperspectral remote sensing in precision agriculture.

Keywords: maize, nitrogen, hyperspectral imagery, vegetation index, UAV, random forest regression, support vector regression

DOI: 10.25165/j.ijabe.20241703.8663

Citation: Cheng Q W, Wu B S, Ye H C, Liang Y Y, Che Y P, Guo A T, et al. Inversion of maize leaf nitrogen using UAV hyperspectral imagery in breeding fields. Int J Agric & Biol Eng, 2024; 17(3): 144–155.

1 Introduction

Maize (*Zea mays* L.) is a globally cultivated staple food crop[1], boasting extensive planting areas and high yields[2]. As reported by China Information News, the maize planting area in China reached 43.07 million hm^2 in 2022, with a total yield of 277.2 million t, second only to the United States[3]. With the development of the deep processing industry, maize has the same economic attributes as ore and crude oil[4], and is an important economic crop and industrial resource[5,6], intimately linked with economic development[7]. Nitrogen (N) plays a dual role as a crucial component influencing the synthesis of proteins, nucleic acids, and chlorophyll in plants[8]. Furthermore, it directly impacts the physiological and biochemical processes of plants[9-11]. During the growth of maize, N deficiency will lead to leaf yellowing or withering, weakening photosynthetic capacity, hampering kernel filling rates, decreasing hundred-grain weight, and ultimately lowering maize yields[12,13]. Therefore, precise and efficient real-time monitoring of maize N's nutritional status is imperative for ensuring normal growth and development of maize and achieving increased and stable yields[14]. Leaf nitrogen content (LNC) is defined as the proportion of total N content in leaves to leaf dry weight, and stands as a crucial indicator reflecting the N nutritional status of crop leaves[15]. However, LNC cannot represent the N nutritional level of the entire plant. Leaf nitrogen accumulation (LNA) as the product of LNC and leaf dry weight[16]. Tan et al.[17] found that LNA not only reflects the N nutritional status of leaves but also encapsulates vegetation coverage characteristics,

Received date: 2023-11-17 **Accepted date:** 2024-03-19

Biographies: Qiwen Cheng, Postgraduate, research interest: remote sensing, Email: 18194294882@163.com; **Bingsun Wu**, PhD, Associate Researcher, research interest: remote sensing, Email: wubingsu11@163.com; **Huichun Ye**, PhD, Associate Researcher, research interest: remote sensing, Email: yehc@aircas.ac.cn; **Yongyi Liang**, Postgraduate, research interest: plant nutrition and fertilization, Email: lyy1017@163.com; **Yingpu Che**, PhD, Postdoctor, research interest: remote sensing, Email: cheyingpu@caas.cn; **Anting Guo**, PhD, Postdoctor, research interest: remote sensing, Email: guoat@aircas.ac.cn; **Zixuan Wang**, Postgraduate, research interest: soil physics, Email: 18005505432@126.com; **Zhiqiang Tao**, PhD, research interest: remote sensing, Email: zhiqiangtao@cau.edu.cn; **Wenwei Li**, Undergraduate, research interest: remote sensing, Email: lvv167678@163.com.

†These authors contributed equally to this work.

***Corresponding author: Jingjing Wang**, PhD, Associate Professor, research interest: remote sensing, Email: pink_wangjing@163.com.

significantly impacting crop yield and seed protein synthesis. Therefore, LNA distinctly reflects the N nutrition status of the entire plant, with monitoring LNA is also of great significance for precision fertilization[18]. In current N nutrition studies, crop N status is predominantly characterized by LNC, utilizing its quantification as a diagnostic tool for evaluating crop N nutrition status[19-22]. However, few studies concurrently select LNC and LNA as monitoring indicators for N nutrition status, comprehensively analyzing the state of plant N nutrition and overall characteristics of plant growth and development, thereby providing a theoretical foundation for the scientific application of N fertilizers and crop management.

Traditional methods for determining crop N content primarily rely on indoor chemical analyses, such as the Kjeldahl method[23,24]. However, field sampling through these methods causes extensive crop damage, necessitates lengthy analysis time, and involves the use of toxic chemical reagents, leading to a time-consuming, labor-intensive, and environmental pollution process[25]. The development of modern remote sensing technology offers the possibility of rapid, non-destructive, and real-time monitoring of crop N status at different scales[26-28]. Studies have shown that remote sensing technology can extract spectral information related to nutrient elements, pigments, and other structural parameters in leaves, thereby estimating different physiological and biochemical indicators of crops[29,30]. Therefore, the use of remote sensing to monitor crop N relies on the link between leaf spectral characteristics and plant physiological and biochemical properties[31]. Currently, remote sensing technology mainly includes two categories: satellite remote sensing and unmanned aerial vehicle (UAV) remote sensing. Due to limited revisit cycles and weather conditions, satellite remote sensing has disadvantages such as low spatial resolution and poor data quality[32,33]. In comparison, UAV remote sensing presents advantages such as lower cost, better timeliness and operability, and higher image resolution[34-36]. As a result, UAV remote sensing finds widespread application in agricultural fields, including seeding[37], pest and disease identification[38,39], crop yield prediction[40,41], and monitoring crop growth indicators[42-44]. The sensors installed on UAV platforms primarily include RGB cameras, multispectral cameras, and hyperspectral images. Among these, hyperspectral images have more bands and higher spectral resolution[45]. This allows them to obtain more precise spectral feature responses, detect subtle changes in ground cover, and exhibit superior performance in monitoring vegetation characteristics[46,47]. Vegetation Indices (VIs) constructed based on canopy spectral reflectance are widely used to study vegetation growth status. Research has found that models established by VIs were more stable[48], making them suitable for crop N inversion. Wen et al.[49] accurately estimated the vertical LNC of maize under different field experimental conditions using the optimized red-edge absorption area index. Guo et al.[50] indicated that the ratio spectral index (NBDI743, NBDI703) had a high accuracy in predicting LNA in spring wheat. Patel et al.[51] evaluated the canopy nitrogen concentration of ryegrass using several VIs, with the results showing that the photochemical reflectance index had a superior predictive effect. Chen et al.[52] found that Medium Resolution Medium Spectrometer (MERIS) Terrestrial Chlorophyll Index (MTCI) and Red Edge Chlorophyll Index ($CI_{red\ edge}$) achieved a higher prediction accuracy of plant nitrogen concentration at the flowering stage of winter wheat. Consequently, the prediction of crop N nutritional status by leveraging the relationship between hyperspectral VIs and crop growth parameters has become a prominent research focus. However, using single VIs to predict N status may ignore the differences in spectral characteristics of hyperspectral data, failing to express most spectral information, and potentially leading to oversaturation in constructing crop N status monitoring models[53]. Machine learning regression, with its capability to describe complex relationships between crop parameters and hyperspectral data, has gradually proven advantageous over linear regression[54,55]. Peng et al.[56] demonstrated that the Random forest regression (RFR) algorithm outperformed linear regression in predicting the nitrogen nutrition index (NNI) of potatoes. Zhang et al.[57] successfully employed RFR and XGBoost regression models to predict the aboveground biomass of maize at different growth stages. Ma et al.[58] utilized multiple VIs to construct a Support Vector Regression (SVR) model for estimating LNC in cotton and achieved favorable prediction results. Yang et al.[59] combined Optimized Spectral Index with four machine learning algorithms, with the RFR combination had high prediction accuracy for N content in plants such as wheat, maize, rice, and potatoes. In the above studies, most of the research subjects were planted in non-tropical regions, there is a scarcity of research using UAV hyperspectral data for real-time monitoring and inversion of maize N nutrient status in tropical regions.

Hainan is a prominent tropical region in China, known for its unique ecological features characterized by early spring onset, rapid warming, significant diurnal temperature variations, and a frost-free climate throughout the year[60]. It has special ecological attributes that meet the year-round, multi-generational, or perennial growth of maize, which is the most important ideal base for southern breeding in China[61]. Therefore, this study took maize in Hainan area as the research object and used LNC and LNA as indicators to characterize the N nutrition status of maize. Typical VIs were constructed using UAV hyperspectral images, and the study analyzed the model accuracy between single VIs and maize leaf N. Multivariable linear regression (MLR), RFR algorithm, and SVR algorithm were used to construct prediction models between important VIs and N indicators. The model with the highest prediction accuracy was applied to invert the LNC and LNA of maize in the study area. The goal is to realize remote sensing estimation of leaf N nutrition status for maize propagated in the southern region. This aims to provide a rapid and effective technical method for non-destructive monitoring of N, assessing the critical stages of maize growth, and making informed decisions about field fertilizer. The ultimate objective is to ensure an ample nitrogen supply, promote maize growth, and achieve stable and increased yields.

2 Materials and methods

2.1 Experimental design

The experiment was conducted at the South Propagation Maize Breeding Base in Laopo Village, Ledong County, Hainan Province, China (18°26′33″N, 108°57′26″E) in January 2022 (Figure 1a). Situated in the southwest of Hainan Island, Ledong County experiences a tropical monsoon climate with sufficient light and distinct dry and wet seasons. The predominant soil type is latosol. The average annual temperature, sunlight hours, and precipitation are 23°C-25°C, 2100-2600 h, and 1400-1800 mm, respectively. The seasonal distribution of precipitation is uneven, with 86% of the annual precipitation concentrated in the wet season from May to October.

Field measurements were conducted to obtain hyperspectral reflectance and LNC data of maize. A total of 76, 2 m×2 m, sampling units were selected and evenly distributed in 2 sampling plots that represented the growth characteristics of maize at the filling stage. The sampling units were randomly divided into two datasets in the ratio of 8:2, with 60 units used for model simulation and 16 units for model validation (Figure 1b). The soil physical and chemical properties in Plot 1 and Plot 2 are listed in Table 1. Besides, the planting density in Plot 1 was 6 plants/m^2, and the planting density in Plot 2 was 7 plants/m^2. The screened 13 important VIs were used as inputs, while LNC and LNA of maize were used as outputs to construct MLR, RFR, and SVR models, respectively. Subsequently, precision tests were conducted to assess the accuracy of the models.

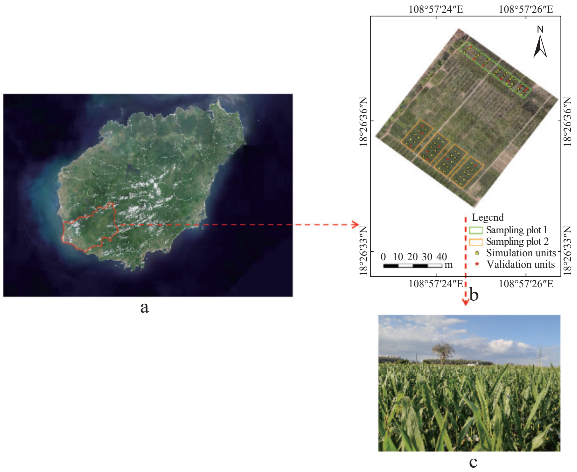

Figure 1 Location of the experimental site and distribution of sampling units

Table 1 Soil physical and chemical properties at sampling plots

Sampling plots	Soil textures	Particle composition/%			Total N content/g·kg^{-1}	
		Clay (<0.002 mm)	Silt (0.002-0.020 mm)	Sand (0.02-2 mm)	Depth (0-20 cm)	Depth (20-40 cm)
Plot 1	Heavy clay	67.21	20.93	11.83	2.75	2.32
Plot 2	Loamy clay	44.13	33.05	22.82	2.35	1.98

2.1.1 Data collection

1) Hyperspectral reflectance measurement

The leaf hyperspectral reflectance of maize at the filling stage was measured using the Jingwei M300 RTK quadcopter UAV equipped with the ULTRIS X20 Plus hyperspectral imager on January 15, 2022, from 11:00 AM to 1:00 PM (Beijing local time) under clear and cloudless weather conditions. The UAV was set to fly at a height of 40 m, with a speed of 5 m/s. The shooting mode was timed shooting, with a shortest interval of 2 s between image acquisitions. Both forward and side overlaps were set to 75%. The wavelength range of the hyperspectral imager was 350-1000 nm, the spatial resolution was 1.5 cm/pixel, and the sampling interval was 4 nm. A total of 164 bands of leaf spectral reflectance data were collected. The instrument was accurately calibrated using a whiteboard before measuring each sampling unit.

2) Determination of leaf N indicator

Maize leaf samples were collected on January 16 and 17, 2022. After the leaf hyperspectral reflectance data were recorded, four representative maize plants near the locations of the spectral measurements were randomly selected in each of the 76 sampling units. Subsequently, maize leaves were collected and quickly transported to the laboratory to determine LNC (%). All green leaves were cleaned and oven-dried at 105°C for 30 min, and then dried at 80°C for 8 h until a constant weight was achieved After crushing, the Kjeldahl method was used to measure the N content of the leaves. Thereafter, the LNA was calculated as the product of LNC and unit leaf dry weight. The statistics for the measured LNC and LNA of maize are listed in Table 2.

$$\text{LNA} = \text{LNC} \times \text{drymatter} \tag{1}$$

where, LNA is the leaf nitrogen accumulation, g/m^2; LNC is the leaf nitrogen content, %; dry matter is the unit leaf dry weight, g/m^2.

Table 2 Descriptive statistics of measured maize LNC (%) and LNA (g/m²) for the simulation and validation datasets at the filling stage

Dataset	Nitrogen indicators	N	Max	Min	Mean	SD	CV
Simulation dataset	LNC	60	2.50	0.77	1.78	0.36	0.20
	LNA		3.39	0.81	1.92	0.58	0.30
Validation dataset	LNC	16	2.26	0.85	1.72	0.37	0.21
	LNA		2.72	0.86	1.84	0.50	0.27

Note: Max, maximum; Min, minimum; SD, standard deviation; CV, coefficient of variation.

2.2 Hyperspectral VIs and data analysis

The hyperspectral VIs commonly used for estimating crop N status are listed in Table 3. The correlation and regression analyses

Table 3 Published hyperspectral VIs evaluated in this study

Vegetation Index	Equation	Reference
Simple ratio (SR) 1	R810/R560	[62]
SR 2	R750/R710	[63]
Ratio Vegetation Index (RVI) 1	R800/R670	[64]
RVI 2	R810/R720	[65]
Normalized Difference Vegetation Index (NDVI)	(R800−R680)/(R800+R680)	[66]
Green Normalized Difference Vegetation Index (GNDVI)	(R800−R550)/(R800+R550)	[67]
Normalized Difference Red Edge Index (NDRE)	(R790−R720)/(R790+R720)	[68]
Enhanced Vegetation Index 2 (EVI 2)	2.5×(R800−R680)/(1+R800+2.4R680)	[69]
Green Chlorophyll Index (CI_{green})	(R780/R550)−1	[70]
Red Edge Chlorophyll Index ($CI_{red\ edge}$)	(R780/R710)−1	[70]
MERIS Terrestrial Chlorophyll Index (MTCI)	(R750−R710)/(R710−R680)	[71]
Modified Red-Edge Normalized Difference Vegetation Index (mND705)	(R750−R705)/(R750+R705−2R445)	[72]
Optimized Soil-adjusted Vegetation Index (OSAVI)	1.16×(R800−R670)/(R800+R670+0.16)	[73]
Modified Chlorophyll Absorption Ratio Index (MCARI)	1.2×[120×(R780−R550)−200×(R800−R550)]	[74]
Transformed Vegetation Index (TVI)	0.5×[120×(R780−R550)−200×(R670−R550)]	[75]
Modified Simple Ratio (MSR)	(R800/R670−1)/sqrt(R800/R670+1)	[76]
Modified Chlorophyll Absorption Vegetation Index (MCAVI)	0.2×[2R800+1−sqrt(2R800+1)×2−8×(R800−R670)]	[77]
Soil Adjusted Vegetation Index (SAVI) 1	1.5×(R800−R670)/(R80+R670+0.5)	[78]
SAVI 2	0.92×(R825−R735)/(R825+R735−0.08)	[78]
Normalized Difference Chlorophyll (NDchl)	(R925−R710)/(R925+R710)	[79]
Normalized Difference Spectral Index (NDSI)	(R788−R756)/(R788+R746)	[80]
Modified Red Edge Ratio (mRER)	(R759−1.8R419)/(R742−1.8R419)	[81]
Red Edge Position (REP)	700+40×[(R670+R780)/2−R700]/(R740−R700)	[82]
New Double Difference (DDN) Index	2R710−R660−R760	[83]

Note: R810 denotes the reflectance at the wavelength of 810 nm in the hyperspectral data, and the same others.

were conducted using SPSS 27.0 software, heat map was conducted with Origin 2021 software. The orthogonal partial least squares-discriminant analysis was processed with SIMCA 14.1 software, and the variable importance in projection (VIP) was calculated. Subsequently, important VIs were screened with VIP>1. The MLR, RFR, and SVR were performed using MATLAB 7.0 software (The MathWorks, Inc., Natick, MA, USA). Model accuracy was assessed using the coefficient of determination (R^2), root mean squared error (RMSE), and relative error (RE, %), as defined by Equations (2)-(4), respectively. A higher R^2 and smaller RMSE and RE indicated better model precision in predicting LNC and LNA.

$$R^2 = 1 - \frac{\sum_{i=1}^{n}(O_i - P_i)^2}{\sum_{i=1}^{n}(O_i - \bar{y})^2} \tag{2}$$

$$\mathrm{RMSE} = \sqrt{\frac{1}{n}\sum_{i=1}^{n}(P_i - O_i)^2} \tag{3}$$

$$\mathrm{RE}\left(\%\right) = \frac{\mathrm{RMSE}}{\bar{y}} \times 100\% \tag{4}$$

where, O_i, P_i, and $\bar{y}$ are the measured values, the predicted values, and the average of the measured values, respectively; n is the number of samples.

3 Results

3.1 Relationship between VIs and LNC, LNA

As listed in Table 4, the 24 hyperspectral VIs were analyzed by linear regression with LNC and LNA, and the corresponding prediction models were established, and then the samples from the validation dataset were applied for validation, The results showed that except for NDVI, GNDVI, NDRE, mND705, SAVI 2, and NDchl, which had higher prediction accuracy for LNC than LNA (R^2≥0.66, RMSE≤0.31, RE≤16.66%), the remaining 18 VIs had higher prediction accuracy for LNC (R^2≥0.55, RMSE≤0.25, RE≤14.32%), with an average R^2 of 0.02 higher than LNA. For estimating LNC, except for the poor prediction accuracy of TVI, MCAVI, and NDSI for LNC (R^2≤0.59, RMSE≥0.23, RE≥13.62%), the remaining 21 VIs had higher prediction accuracy for LNC (R^2≥0.61, RMSE≤0.23, RE≤13.30%). For estimating LNC, the 5 highest prediction accuracy VIs were NDchl, mRER, SR 1, NDRE, and RVI 2 (R^2≥0.69, RMSE≤0.21, RE≤12.37%). For estimating LNA, the poor prediction accuracy VIs were EVI 2, MCARI, TVI, MCAVI and NDSI (R^2≤0.59, RMSE≥0.33, RE≥18.16%), while NDchl, mRER, NDRE, GNDVI and mND705 had higher prediction accuracy for LNA (R^2≥0.70, RMSE≤0.29, RE≤15.89%).

Table 4 Quantitative relationships of VIs to LNC and LNA in maize

Spectral index	LNC			LNA		
	R^2	RMSE	RE	R^2	RMSE	RE
SR 1	0.71	0.21	12.21%	0.69	0.30	16.45%
SR 2	0.68	0.21	12.46%	0.66	0.32	17.23%
RVI 1	0.65	0.22	12.94%	0.62	0.33	17.94%
RVI 2	0.69	0.21	12.37%	0.68	0.31	16.70%
NDVI	0.63	0.23	13.27%	0.66	0.30	16.56%
GNDVI	0.67	0.22	12.64%	0.71	0.29	15.83%
NDRE	0.70	0.21	12.23%	0.71	0.29	15.78%
EVI 2	0.61	0.23	13.07%	0.59	0.33	18.16%
CI_{green}	0.68	0.21	12.40%	0.67	0.31	16.90%
$CI_{red\ edge}$	0.66	0.22	12.66%	0.65	0.32	17.53%
MTCI	0.66	0.22	12.89%	0.65	0.32	17.17%
mND_{705}	0.68	0.22	12.47%	0.70	0.29	15.89%
OSAVI	0.63	0.22	12.87%	0.63	0.31	17.09%
MCARI	0.61	0.22	12.97%	0.57	0.34	18.62%
TVI	0.55	0.24	13.91%	0.52	0.36	19.43%
MSR	0.65	0.22	12.82%	0.65	0.32	17.45%
MCAVI	0.57	0.23	13.62%	0.53	0.36	19.45%
SAVI 1	0.61	0.22	13.02%	0.60	0.33	17.90%
SAVI 2	0.67	0.23	13.30%	0.69	0.31	16.66%
NDchl	0.72	0.21	12.19%	0.77	0.26	14.34%
NDSI	0.59	0.25	14.32%	0.55	0.37	19.86%
mRER	0.72	0.21	12.14%	0.72	0.29	15.64%
REP	0.65	0.22	13.02%	0.65	0.31	16.91%
DDN	0.65	0.22	12.50%	0.63	0.32	17.47%

3.2 Selection of VIs for evaluating LNC and LNA

In order to predict LNC and LNA of maize more accurately, the orthogonal partial least squares-discriminant analysis was performed on LNC, LNA, and different VIs were calculated VIP values. By comparison, all VIs were classified into 2 categories, important variables (VIP>1), and unimportant variables (VIP≤1). The results are shown in Figure 2. Among the 24 VIs, the maximum VIP value of MTCI was 1.027, while the minimum VIP value of TVI was 0.950. A total of 11 unimportant variables were screened out, including NDVI, EVI 2, mND705, OSAVI, MCARI, TVI, MCAVI, SAVI 1, SAVI 2, NDchl and NDSI, with VIP values of 0.950-1.000. The remaining 13 VIs, including SR 1, SR 2, RVI 1, RVI 2, GNDVI, NDRE, CI_{green}, $CI_{red\ edge}$, MTCI, MSR, mRER, REP, and DDN were selected as important variables, with VIP values of 1.002-1.027.

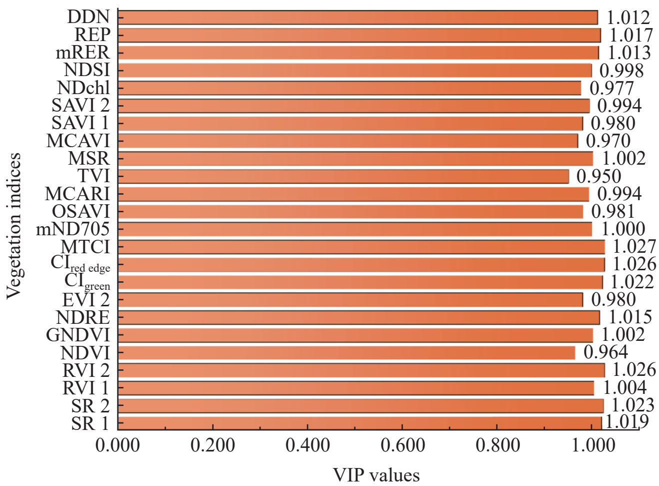

Figure 2 VIP values of 24 VIs

As shown in Figure 3, the correlation analysis was conducted on the 13 important variables and LNC and LNA. The results showed that all VIs had strong correlations with LNC and LNA, with absolute values of their determination coefficients above 0.70, and reached highly significant correlations at the 0.01 level. Compared with LNC, the correlation between the 13 important VIs and LNA was higher, and the absolute values of their determination coefficients were higher than that of LNC by 0.04 on average. Among the 13 important VIs, only DDN showed a significant positive correlation with LNC and LNA (p<0.01), and had the highest correlation with both LNC and LNA, with correlation coefficients of 0.77 and 0.82, respectively. The remaining vegetation indices were all significantly negatively correlated with

LNC and LNA (p<0.01). The 5 VIs with the best correlation with LNC were DDN, SR 2, $CI_{red\ edge}$, RVI 1, and MSR, with absolute determination coefficients of 0.77-0.79, while the 5 VIs with the lowest correlation with LNC were REP, GNDVI, mRER, NDRE, and MTCI, with absolute determination coefficients of 0.73-0.76. The 5 VIs with the best correlation with LNA were DDN, SR 2, RVI 1, MSR, and $CI_{red\ edge}$, with absolute determination coefficients of 0.82-0.84, while the 5 VIs with the lowest correlation with LNA were REP, mRER, MTCI, GNDVI, and NDRE, with absolute determination coefficients of 0.74-0.79.

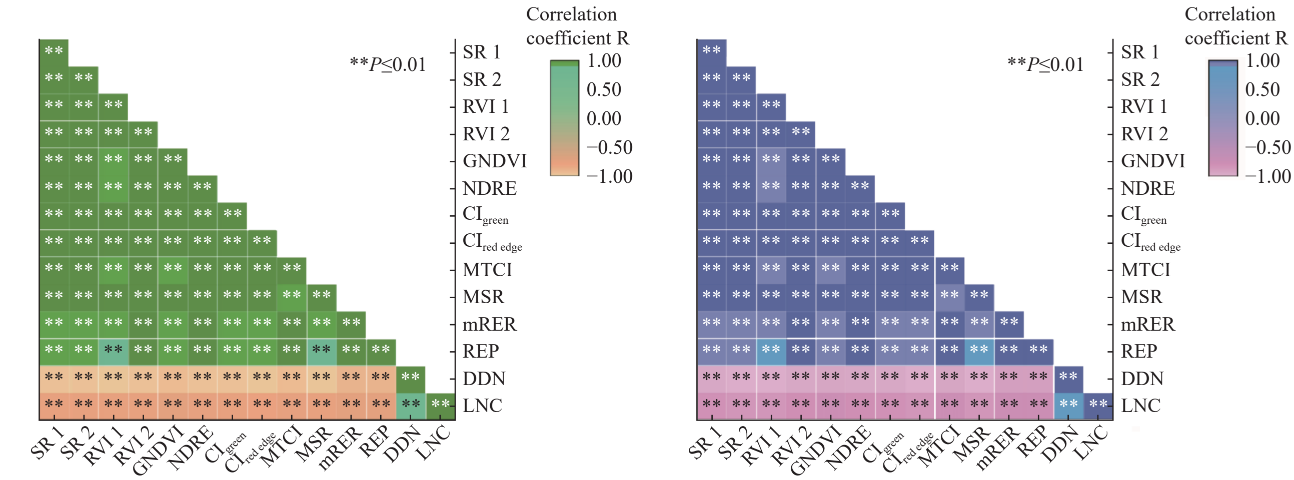

a. correlation correlations between important variables and LNC

b. Correlation correlations between important variable and LNA

Figure 3 Correlation coefficients between 13 important variables and LNC, LNA in maize

3.3 Comparison and testing of model estimation accuracy

Based on the above-selected important variables, MLR, RFR, and SVR were used to establish the monitoring models for LNC and LNA of maize, respectively. R^2, RMSE, and RE values were used to compare and analyze the consistency between the predicted and observed values of LNC and LNA in the simulation and validation datasets modeled by different algorithms, and then the accuracy of the monitoring models was evaluated. As shown in Figure 4, compared to the single linear regression model (LNC: R^2≥0.55, RMSE≤0.25, RE≤14.32%; LNA: R^2≥0.52, RMSE≤0.37, RE≤ 19.86%), the MLR model did not significantly improve the prediction accuracy of LNC (simulation dataset: R^2=0.70, RMSE= 0.19, RE=10.89%; validation dataset: R^2=0.59, RMSE=0.24, RE=13.83%) and LNA (simulation dataset: R^2=0.77, RMSE=0.28, RE=14.38%; validation dataset: R^2=0.53, RMSE=0.38, RE=20.58%). Among the 4 different models, the RFR model had the highest prediction accuracy for LNC (simulation dataset: R^2=0.82, RMSE=0.16, RE=8.95%; validation dataset: R^2=0.78, RMSE=0.16, RE=8.83%) and LNA (simulation dataset: R^2=0.84, RMSE=0.23, RE=12.41%; validation dataset: R^2=0.85, RMSE=0.19, RE=9.88%). In addition, the SVR model also had good prediction accuracy. For LNC, its R^2 and RMSE values of the validation dataset were the same as the RFR model, but the RE value was 0.42% higher than the RFR model. The R^2 value of the simulation dataset was 0.12 lower than the RFR model, and the RMSE and RE values were 0.04 and 2.52% higher, respectively. For LNA, its prediction accuracy was significantly lower than that of the RFR model (simulation dataset: R^2=0.78, RMSE=0.27, RE=14.02%; validation dataset: R^2=0.73, RMSE=0.26, RE=13.89%).

3.4 Mapping of LNC and LNA in the study area

The RFR model with the highest prediction accuracy was selected and used 76 sampling units as the basic unit, and then LNC and LNA for each sampling unit were predicted separately, the inversion results are shown in Figure 5. Overall, the changes in LNC and LNA at the sampling unit scale were basically consistent. The predicted values of LNA in the study area were all higher than the predicted values of LNC. The minimum predicted value of LNC was 1.23%, the maximum was 2.17%, and the average value was 1.76%. The minimum predicted value of LNA was 1.24 g/m^2, the maximum was 2.72 g/m^2, and the average value was 1.89 g/m^2. In addition, the soil of sampling Plot 1 was heavy clay, while sampling Plot 2 was loamy clay, and the soil total N content in 0-20 cm and 20-40 cm layers was higher than that in sampling Plot 2 (Table 1). Besides, the planting density of maize in sampling Plot 1 was lower than that in sampling Plot 2. The results of the study showed that the predicted values of LNC and LNA in sampling Plot 1 were higher than that in sampling Plot 2.

4 Discussion

4.1 Relationship between VIs and LNC and LNA

The estimation of maize LNC and LNA based on linear regression is primarily constructed through a simple empirical regression model from VIs in narrow hyperspectral bands[84]. In this study, 24 commonly used VIs were used to establish predictive models for maize LNC and LNA. Table 4 presents the prediction accuracy of single VIs for LNC and LNA, with most VIs having R^2 values above 0.60. This indicates that VIs composed of narrow bands of reflectance can mitigate interference caused by soil, weather, and other factors, thereby enhancing the accuracy of crop parameter estimation[52]. Song et al.[85] found that NDRE, mRER, and NDchl had high accuracy in predicting N accumulation during the flowering stage of wheat (R^2≥0.75, RMSE≤0.32). In this study, NDRE, mRER, and NDchl not only had the highest prediction accuracy for maize LNA (R^2≥0.71, RMSE≤0.29, RE≤15.78%), but also had high accuracy for LNC (R^2≥0.70, RMSE≤0.21, RE≤ 12.23%). This suggests that NDRE, mRER, and NDchl can be effective VIs for estimating crop N status. The REP is believed to partially eliminate effects caused by canopy structure and soil background[86-88]. Ramos-García et al.[89] demonstrated that REP is suitable for monitoring the N nutrition status of maize leaves during the eighth leaf stage (R^2=0.46) and silking stage (R^2=0.54). In this study, REP had higher predictive accuracy for LNC and LNA (R^2=0.65) during the filling stage of maize, indicating that REP can be a suitable indicator for estimating the N nutrition status of maize

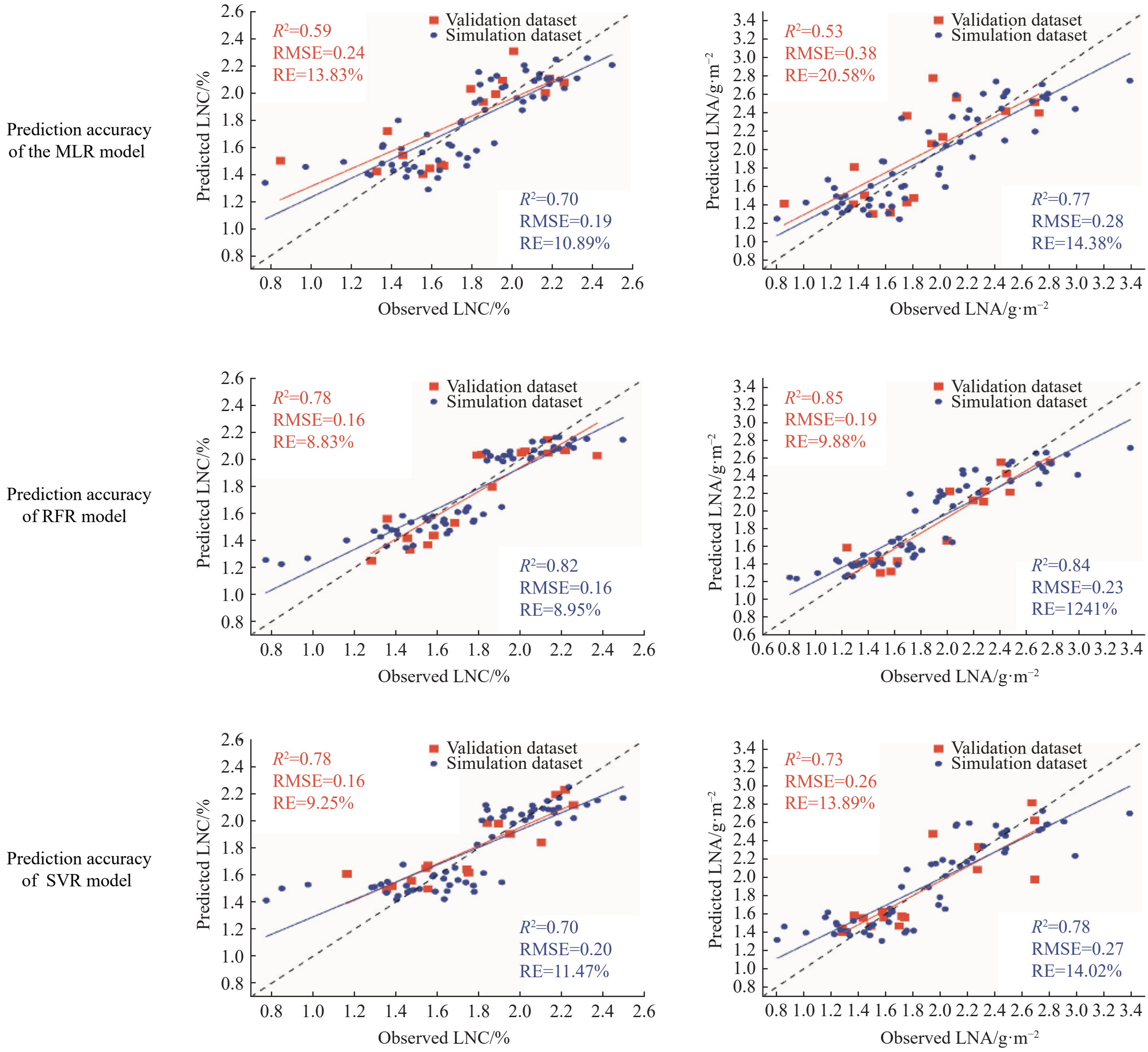

a. LNC b. LNA

Figure 4 Comparison of accuracy of different prediction models for LNC and LNA in maize

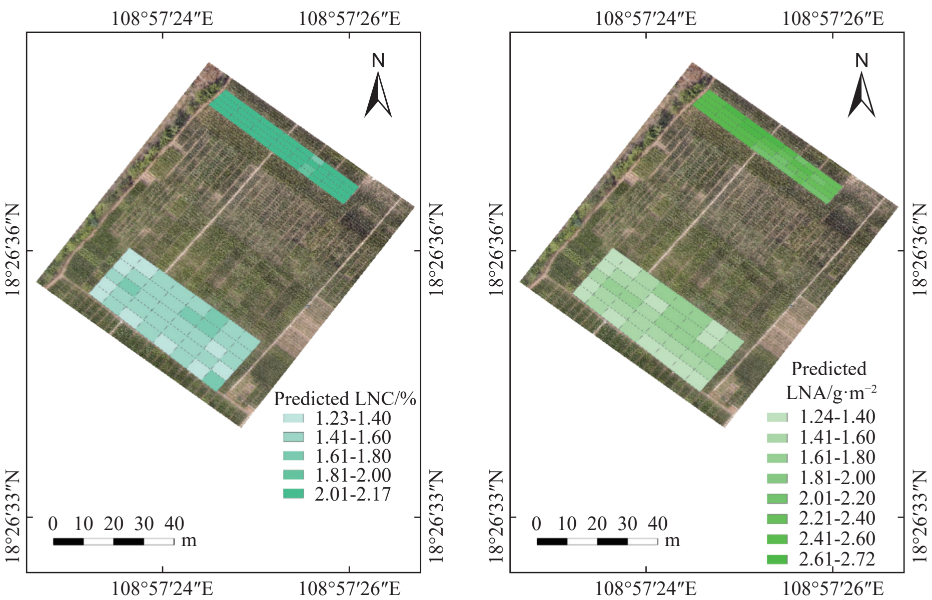

a. LNC b. LNA

Figure 5 Mapping of LNC and LNA in maize based on the optimal estimation model at different growth stages. Additionally, due to the increase in leaf density and decrease in leaf transparency during the filling stage, REP is more sensitive to changes in leaf structure[90,91], resulting in higher prediction accuracy for the N nutrition status of maize. Numerous studies have shown that TVI is often used to estimate the leaf area index of crops[92-94] and has achieved good prediction accuracy (R^2=0.53-0.96). However, in this study, TVI failed to exhibit high prediction accuracy for LNC (R^2=0.55, RMSE=0.24, RE=13.91%) and LNA (R^2=0.52, RMSE=0.36, RE=19.43%). The reason may be that TVI has a weak ability to monitor changes in factors affecting N content, such as canopy structure and functional traits[95], and its inability to directly reflect the N status in leaves, resulting in poorer prediction accuracy. In this study, MCAVI had poor prediction accuracy for LNC (R^2=0.57, RMSE=0.23, RE=13.62%) and LNA (R^2=0.53, RMSE=0.36, RE=19.45%). Studies have shown that the canopy spectral reflectance of crops is determined by the optical properties of leaves and the surrounding environment[96,97]. The cellular structure, moisture, and leaf thickness inside maize leaves can cause light scattering and cross-reflection within the leaves[98,99], affecting the accuracy of MCAVI in predicting leaf N and resulting in poor predictions. NDVI as a vegetation index highly correlated with crop N content[100-102], has been widely used in monitoring crop N status[103-106].Ye et al.[107] used 12 VIs to estimate leaf N density of maize with different geometrical traits at different growth stages, among which NDVI had the highest accuracy in predicting the upper leaves of horizontal maize (R^2=0.83) and intermediate maize (R^2=0.57) during the period of an unclosed canopy. However, in this study, NDVI, and NDSI did not exhibit high prediction accuracy for LNC (R^2≤0.63, RMSE≥0.23, RE≥13.27%) and LNA (R^2≤0.66, RMSE≥0.30, RE≥16.56%). This discrepancy may be attributed to the sensitivity of these types of VIs to changes in soil background, which are easily influenced by factors such as wavelength, vegetation coverage, light intensity, and soil characteristics like water content, organic matter content, and surface roughness[108]. They only consider the spectral reflectance characteristics of vegetation and do not account for the comprehensive impact of these factors, resulting in low prediction accuracy for maize leaf N. To reduce the influence of non-photosynthetic substances in the canopy on reflectance spectra, Sims and Gamon[109] developed a three-band vegetation index, mND705. In this study, the predictive performance of mND705 for both LNC and LNA showed improvement compared to NDSI, with an increase in R^2 values by 0.09 and 0.15, RMSE and RE values decreased by 0.03, 0.08 and 1.85%, 3.97%, respectively. This proves that the three-band vegetation index contains more detailed vegetation information, enhances the sensitivity of crop physiological and biochemical indicators, reduces the influence of external environmental conditions, and consequently improves the prediction accuracy of crop parameters[110].

4.2 The best model for monitoring LNC and LNA

In this study, the single vegetation index-based estimation model for LNC and LNA demonstrated good accuracy. However, models constructed by single VIs are susceptible to saturation[111] and have limited sensitivity to changes in crop internal and canopy structure[112]. In order to enhance sensitivity to parameters like LNC and LNA, this study calculated VIP values and screened 13 important VIs with VIP>1 (Figure 2). Correlation analysis was then conducted on these 13 VIs with LNC and LNA, respectively (Figure 3). The results revealed that only DDN was significantly positively correlated with LNC (r=0.79) and LNA (r=0.84), aligning with previous research findings[113]. Fan et al.[114] reported higher correlation coefficients between VIs and N indexes involving the red band and the red-edge band, with absolute values of their correlation coefficients all above 0.80. Additionally, REP was significantly negatively correlated with LNC (r=−0.73) and LNA (r=−0.74), primarily due to the close correlation between N and chlorophyll content in crops[115-117]. Machine learning regression has gained widespread use in estimating crop physiological and biochemical indicators, demonstrating promising potential[118-123]. In this study, 13 important VIs served as input variables for the quantitative estimation of maize LNC and LNA from hyperspectral images, using single linear regression, multivariable linear regression, and machine learning regression. Figure 4 illustrates the predictive performances of the MLR, RFR, and SVR models for maize LNC and LNA. The results indicated that compared to single linear regression models, multivariable linear regression did not significantly improve the prediction accuracy of both LNC and LNA, consistent with previous research results[52]. This is because MLR cannot deal with problems such as multicollinearity in spectral data and is only suitable for solving some linear regression problems, resulting in lower model accuracy[124,125]. In contrast, the machine learning-based RFR model and SVR model have higher prediction accuracy for maize LNC and LNA. Wang et al.[126] demonstrated that RFR (R^2=0.63-0.74) and SVMR (R^2=0.59-0.70) models have higher prediction accuracy for rice leaf area index, aligning with the conclusion that SVMR and RFR models can provide better prediction results in this study. Fu et al.[102] emphasized that complexity and nonlinearity characterize the relationship between hyperspectral reflectance and crop N status. Additionally, there are often significant nonlinear relationships between VIs and crop parameters. Therefore, machine learning models are better suited for capturing the nonlinear relationships between various VIs and crop parameters[127]. Consequently, both machine learning algorithms in this study demonstrated superior prediction performance. The RFR algorithm is based on numerous decision trees and nonlinear regression trained on high dimensional data to achieve calculations on extensive datasets[128,129], It exhibits low sensitivity to data bias[130], can model complex variables through interactions to prevent overfitting[131], and is widely used in various remote sensing based analyses due to its robustness, stability, high predictability, fast training speed and ease of implementation[132,133]. Shah et al.[134] showed that compared to MLR (R^2=0.86, RMSE=6.04), the use of RFR to predict wheat chlorophyll content resulted in an increased R^2 and decreased RMSE (R^2=0.95, RMSE=3.71). Qiu et al.[135] compared the predictive performance of different machine learning methods on the NNI of rice, and reported that the RFR algorithm had the highest accuracy in predicting the NNI at each growth stage (R^2=0.88-0.96, RMSE=0.03-0.07). Sun et al.[136] showed that in predicting the canopy chlorophyll content of wheat and soybeans, RFR (R^2=0.69-0.99) outperformed univariate linear regression (R^2=0.69-0.90) and bivariate linear regression (R^2=0.69-0.82) models. Consistent with previous studies[137-139], the results of this study also indicated that the RFR model had the highest prediction accuracy for LNC and LNA, highlighting the RFR algorithm as the preferred method for predicting LNC and LNA in maize.

4.3 Inversion of N status in maize leaves in the study area

Leaves are a key part of plant photosynthesis, and N in leaves serves as a vital parameter for enhancing light use efficiency, photosynthesis rate, and crop productivity[140,141]. The estimation of N status in the late stages of crop growth holds great significance for predicting maize grain yield and quality, as well as prospects for the following year's crops[142]. The RFR model was employed to invert the LNC and LNA of maize in the study area (Figure 5), and the results showed that the LNC value at the filling stage was 1.23%-2.17%, and the LNA value was 1.24 g/m^2-2.72 g/m^2. Wen et al.[143] also showed that the LNC in maize at the reproductive growth stages (silking stage and milk stage were 0.73%-2.06%, 0.49%-2.21%, respectively) were maintained at a lower level compared to the LNC at the vegetative growth stages (V9 stage and VT stage were 1.10%-4.07%, 1.10%-2.72%, respectively). This is in agreement with the results of this study, indicating that different growth stages have an impact on N changes in maize leaves. The phenomenon might be attributed to the abundance of N content in nutrient tissues during the vegetative growth stages. In contrast, during the reproductive growth stages (filling stage in this paper), owing to grain formation, N in the leaves is transferred to the grains, maintaining a high level of N nutrition in the grains to ensure normal maize fruiting[144-146]. Moreover, N in leaves during the filling stage may be lost from plant tissues in the form of NH3, resulting in a reduction in leaf N nutrition, so that the LNC and LNA in maize are maintained at a low level. Lu et al.[147] showed that the LNC of maize during the filling stage was 1.45%-2.38%, which was higher than the LNC of this study. As the most direct source of crop growth and nutrients, changes in soil nutrient status directly impact the nutrient content of crops[148]. Given that this study was conducted in a tropical region, the high temperature and humidity conditions led to strong soil leaching, resulting in substantial nutrient loss from the soil[149]. This contributed to the low N content observed in maize leaves. Additionally, the soil in the Hainan Island region has an obvious acidification phenomenon[150], which to some extent inhibits microbial activities, hampers the decomposition of organic matter, and slows down the release rate of soil nutrients. This may affect the absorption and utilization of N in the soil by plants. The inversion results of this study showed that the maize LNC and LNA were higher in sampling Plot 1 than in sampling Plot 2, potentially influenced by the different physical and chemical properties of the soil in the two plots. As shown in Table 1, Plot 1 was heavy clay soil, while Plot 2 was loamy clay soil. Numerous studies emphasized that soil texture, as a fundamental physical soil property, not only dictates soil fertility but also significantly influences crop growth and N status[151-153]. Heavy clay, with a higher proportion of clay particles compared to loamy clay, possesses robust adsorption and water and fertilizer retention characteristics, fostering favorable conditions for crop growth and nutrient absorption. The content of N in the soil also plays a pivotal role in plant growth, with higher total N content in the soil providing a more favorable environment for sufficient N supply to plants, thereby promoting N accumulation in leaves. In this study, the total N content in both 0-20 cm and 20-40 cm soil layers indicated that Plot 1 was higher than Plot 2. Consequently, the inversion results demonstrated that the LNC and LNA of maize in Plot 1 were higher than those in Plot 2. In addition, planting density emerges as another critical factor influencing maize growth and development. Numerous studies have shown that high planting density can diminish canopy light transmittance, and intensify resource competition among individual maize plants, thereby affecting photosynthesis, nutrient accumulation and distribution, and restricting overall crop growth and development[154,155]. In this study, the higher planting density in Plot 2 (7 plants/m^2) compared to Plot 1 (6 plants/m^2) may have led to inadequate nutrient supply and soil nutrient depletion, resulting in a lack of N in maize leaves. Consequently, the LNC and LNA of maize in Plot 2 were lower than those in Plot 1.

In this study, the experimental focus was solely on maize at the filling stage, and it is acknowledged that different growth stages can significantly influence the relationship between hyperspectral VIs, LNC, and LNA. Nevertheless, employing a combination of 13 important VIs, this study successfully utilized the RFR algorithm and the SVR algorithm to accurately estimate LNC and LNA, achieving high prediction accuracy. The results of this study lay a foundation for non-destructive and real-time monitoring of N content and fertilization management in the propagation of southern maize in Hainan. Future endeavors will contemplate conducting remote sensing quantitative inversion of LNC and LNA in maize using UAV hyperspectral under different growth stages and N application conditions. The VIs and monitoring models applied in this study will be further tested and improved across a wider range of conditions to enhance the accuracy and reliability of the monitoring models.

5 Conclusions

In this study, UAV hyperspectral remote sensing technology was employed to establish prediction models for LNC and LNA during the filling stage of maize in tropical regions. Single linear regression, multivariable linear regression (MLR), and machine learning regression (RFR and SVR) were employed. The results of single linear regression showed that the prediction performances of 24 VIs for LNC and LNA were relatively stable, with NDchl having the highest predictive accuracy for LNC (R^2, RMSE, and RE were 0.72, 0.21, and 12.19%, respectively) and LNA (R^2, RMSE, and RE were 0.77, 0.26 and 14.34%, respectively). To enhance the sensitivity in predicting LNC and LNA, 24 VIs were divided into 13 important VIs and 11 unimportant VIs, and 13 screened important VIs were used as input values. The results showed that RFR and SVR significantly improved prediction accuracy of LNC and LNA compared to single and multivariable linear regression, in which RFR had the highest prediction accuracy for LNC (simulation dataset: R^2=0.82, RMSE=0.16, RE=8.95%; validation dataset: R^2=0.78, RMSE=0.16, RE=8.83%) and LNA (simulation dataset: R^2=0.84, RMSE=0.23, RE=12.41%; validation dataset: R^2=0.85, RMSE=0.19, RE=9.88%). Therefore, based on the hyperspectral reflectance data from UAV, the RFR model enabled effective estimation of maize LNC and LNA. This approach is applicable in precision agriculture, providing a theoretical basis and technical methodology for real-time monitoring of maize N status in the field and achieving scientific fertilization.

Acknowledgements

This work was financially supported by the Hainan Province Science and Technology Special Fund (Grant No. ZDYF2021GXJS038 and Grant No. ZDYF2024XDNY196), Hainan Provincial Natural Science Foundation of China (Grant No. 320RC486), the National Natural Science Foundation of China (Grant No. 42167011).

[References]

[1] Saeed M S, Saeed A. Health benefits of maize crop - An overview. Current Research in Agriculture and Farming, 2020; 1(3): 5–8.

[2] Lai Z L, Fan J L, Yang R, Xu X Y, Liu L J, Li S E, et al. Interactive effects of plant density and nitrogen rate on grain yield, economic benefit, water productivity and nitrogen use efficiency of drip-fertigated maize in northwest China. Agricultural Water Management, 2022; 263: 107453.

[3] Anonymous. Statistical Bulletin on National Economic and Social

Development of the People's Republic of China in 2022. Available:http://www.stats.gov.cn/sj/zxfb/202302/t20230228_1919011.html. Accessed on [2023-02-28].

[4] Gezahegn A M. Role of integrated nutrient management for sustainable maize production. International Journal of Agronomy, 2021; 2021: 9982884.

[5] Rogers A R, Dunne J C, Romay C, Bohn M, Buckler E S, Ciampitti I A, et al. The importance of dominance and genotype-by-environment interactions on grain yield variation in a large-scale public cooperative maize experiment. G3, 2021; 11(2): jkaa050.

[6] Xia Y H, Li J, Hao P H, Wang K, Lei B, Li H L, et al. Discovery of root-lesion nematode (*Pratylenchus scribneri*) on corn in Hainan province of China. Plant Disease, 2022; 106(7): 1999.

[7] Han E Z, Huang Q Y. Global commodity markets, Chinese demand for maize, and deforestation in Northern Myanmar. Land, 2021; 10(11): 1232.

[8] Miao X X, Miao Y, Liu Y, Tao S H, Zheng H B, Wang J M, et al. Measurement of nitrogen content in rice plant using near infrared spectroscopy combined with different PLS algorithms. Spectrochimica Acta Part A: Molecular and Biomolecular Spectroscopy, 2023; 284: 121733.

[9] Mekonnen H, Kibret M. The roles of plant growth promoting rhizobacteria in sustainable vegetable production in Ethiopia. Chemical and Biological Technologies in Agriculture, 2021; 8: 15.

[10] Win K T, Oo A Z, Yokoyama T. Plant growth and yield response to salinity stress of rice grown under the application of different nitrogen levels and *Bacillus pumilus* Strain TUAT-1. Crops, 2022; 2(4): 435–444.

[11] Nasar J, Khan W, Khan M Z, Gitari H I, Gbolayori J F, Moussa A A, et al. Photosynthetic activities and photosynthetic nitrogen use efficiency of maize crop under different planting patterns and nitrogen fertilization. Journal of Soil Science and Plant Nutrition, 2021; 21: 2274–2284.

[12] Xu X G, Fan L L, Li Z H, Meng Y, Feng H K, Yang H, et al. Estimating leaf nitrogen content in corn based on information fusion of multiple-sensor imagery from UAV. Remote Sensing, 2021; 13(3): 340.

[13] Yan S C, Wu Y, Fan J L, Zhang F C, Qiang S C, Zheng J, et al. Effects of water and fertilizer management on grain filling characteristics, grain weight and productivity of drip-fertigated winter wheat. Agricultural Water Management, 2019; 213: 983–995.

[14] Zhang C, Rees R M, Ju X T. Cropping system design can improve nitrogen use efficiency in intensively managed agriculture. Environmental Pollution, 2021; 280: 116967.

[15] Shi P H, Wang Y, Xu J M, Zhao Y L, Yang B L, Yuan Z Q, et al. Rice nitrogen nutrition estimation with RGB images and machine learning methods. Computers and Electronics in Agriculture, 2021; 180: 105860.

[16] Sun H, Feng M C, Yang W D, Bi R T, Sun J J, Zhao C Q, et al. Monitoring leaf nitrogen accumulation with optimized spectral index in winter wheat under different irrigation regimes. Frontiers in Plant Science, 2022; 13: 913240.

[17] Tan C W, Du Y, Zhou J, Wang D L, Luo M, Zhang Y J, et al. Analysis of different hyperspectral variables for diagnosing leaf nitrogen accumulation in wheat. Frontiers in Plant Science, 2018; 9: 674.

[18] Chu X, Guo Y J, He J Y, Yao X, Zhu Y, Cao W X, et al. Comparison of different hyperspectral vegetation indices for estimating canopy leaf nitrogen accumulation in rice. Agronomy Journal, 2014; 106(5): 1911–1920.

[19] Pan Y Y, Wu W X, Zhang J W, Zhao Y J, Zhang J Y, Gu Y Y, et al. Estimating leaf nitrogen and chlorophyll content in wheat by correcting canopy structure effect through multi-angular remote sensing. Computers and Electronics in Agriculture, 2023; 208: 107769.

[20] Cao C L, Wang T L, Gao M F, Li Y, Li D D, Zhang H J. Hyperspectral inversion of nitrogen content in maize leaves based on different dimensionality reduction algorithms. Computers and Electronics in Agriculture, 2021; 190: 106461.

[21] Duan D D, Zhao C J, Li Z H, Yang G J, Yang W D. Estimating total leaf nitrogen concentration in winter wheat by canopy hyperspectral data and nitrogen vertical distribution. Journal of Integrative Agriculture, 2019; 18(7): 1562–1570.

[22] Berger K, Verrelst J, Féret J B, Wang Z, Wocher M, Strathmann M, et al. Crop nitrogen monitoring: Recent progress and principal developments in the context of imaging spectroscopy missions. Remote Sensing of Environment, 2020; 242: 111758.

[23] Chapman H D, Pratt P F. Methods of analysis for soils, plants and waters. Soil Science, 1962; 93(1): 68.

[24] Foomani K S, Abadi S A V, Kavoosi M, Zakerin H, Yazdani M. The effect of periodic irrigation and different amounts of nitrogen fertilizer on yield and yield components of rice. Communications in Soil Science and Plant Analysis, 2020; 52(1): 22–31.

[25] Chlingaryan A, Sukkarieh S, Whelan B. Machine learning approaches for crop yield prediction and nitrogen status estimation in precision agriculture: A review. Computers and Electronics in Agriculture, 2018; 151: 61–69.

[26] Li Z H, Li Z H, Fairbairn D, Li N, Xu B, Feng H K, et al. Multi-LUTs method for canopy nitrogen density estimation in winter wheat by field and UAV hyperspectral. Computers and Electronics in Agriculture, 2019; 162: 174–182.

[27] Fu Y Y, Yang G J, Li Z H, Song X Y, Li Z H, Xu X G, et al. Winter wheat nitrogen status estimation using UAV-based RGB imagery and gaussian processes regression. Remote Sensing, 2020; 12(22): 3778.

[28] Xu S Z, Xu X G, Blacker C, Gaulton R, Zhu Q Z, Yang M, et al. Estimation of leaf nitrogen content in rice using vegetation indices and feature variable optimization with information fusion of multiple-sensor images from UAV. Remote Sensing, 2023; 15(3): 854.

[29] Kira O, Linker R, Gitelson A. Non-destructive estimation of foliar chlorophyll and carotenoid contents: Focus on informative spectral bands. International Journal of Applied Earth Observation and Geoinformation, 2015; 38: 251–260.

[30] Hunt Jr E R, Doraiswamy P C, McMurtrey J E, Daughtry C S T, Perry E M, Akhmedov B. A visible band index for remote sensing leaf chlorophyll content at the canopy scale. International journal of applied earth observation and Geoinformation, 2013; 21: 103–112.

[31] Abulaiti Y, Sawut M, Maimaitiaili B, Chunyue M. A possible fractional order derivative and optimized spectral indices for assessing total nitrogen content in cotton. Computers and Electronics in Agriculture, 2020; 171: 105275.

[32] Tao H H, Feng H K, Xu L J, Miao M K, Long H L, Yue J B, et al. Estimation of crop growth parameters using UAV-based hyperspectral remote sensing data. Sensors, 2020; 20(5): 1296.

[33] Monforte P, Ragusa M A. Temperature trend analysis and investigation on a case of variability climate. Mathematics, 2022; 10(13): 2202.

[34] Jin X L, Zarco-Tejada P J, Schmidhalter U, Reynolds M P, Hawkesford M J, Varshney R K, et al. High-throughput estimation of crop traits: A review of ground and aerial phenotyping platforms. IEEE Geoscience and Remote Sensing Magazine, 2020; 9(1): 200–231.

[35] Jung H J, Tajima R, Ye R L, Hashimoto N, Yang Y, Yamamoto S, et al. Utilization of UAV remote sensing in plant-based field experiments: A case study of the evaluation of LAI in a small-scale sweetcorn experiment. Agriculture, 2023; 13(3): 561.

[36] Delavarpour N, Koparan C, Nowatzki J, Bajwa S, Sun X. A technical study on UAV characteristics for precision agriculture applications and associated practical challenges. Remote Sensing, 2021; 13(6): 1204.

[37] Liu W, Zou S S, Xu X L, Gu Q Y, He W Z, Huang J, et al. Development of UAV-based shot seeding device for rice planting. Int J Agric & Biol Eng, 2022; 15(6): 1–7.

[38] Bouguettaya A, Zarzour H, Kechida A, Taberkit A M. A survey on deep learning-based identification of plant and crop diseases from UAV-based aerial images. Cluster Computing, 2023; 26(2): 1297–1317.

[39] Mothapo M C, Dube T, Abdel-Rahman E, Sibanda M. Progress in the use of geospatial and remote sensing technologies in the assessment and monitoring of tomato crop diseases. Geocarto International, 2022; 37(16): 4784–4804.

[40] Lukas V, Huňady I, Kintl A, Mezera J, Hammerschmiedt T, Sobotková J, et al. Using UAV to identify the optimal vegetation index for yield prediction of oil seed rape (*Brassica napus* L.) at the flowering stage. Remote Sensing, 2022; 14(19): 4953.

[41] Cheng E H, Zhang B, Peng D L, Zhong L H, Yu L, Liu Y, et al. Wheat yield estimation using remote sensing data based on machine learning approaches. Frontiers in Plant Science, 2022; 13: 1090970.

[42] Gong Y, Yang K L, Lin Z H, Fang S H, Wu X T, Zhu R S, et al. Remote estimation of leaf area index (LAI) with unmanned aerial vehicle (UAV) imaging for different rice cultivars throughout the entire growing season. Plant Methods, 2021; 17(1): 88.

[43] Yue J B, Feng H K, Li Z H, Zhou C Q, Xu K J. Mapping winter-wheat biomass and grain yield based on a crop model and UAV remote sensing. International Journal of Remote Sensing, 2021; 42(5): 1577–1601.

[44] Wang Q, Che Y P, Shao K, Zhu J Y, Wang R L, Sui Y, et al. Estimation of sugar content in sugar beet root based on UAV multi-sensor data. Computers and Electronics in Agriculture, 2022; 203: 107433.

[45] Zhou Y M, Jiang M J. Comparison of inversion method of maize leaf area index based on UAV hyperspectral remote sensing. Multimedia Tools and Applications, 2020; 79: 16385–16401.

[46] Lu B, Dao P D, Liu J G, He Y H, Shang J L. Recent advances of hyperspectral imaging technology and applications in agriculture. Remote Sensing, 2020; 12(16): 2659.

[47] Guo A T, Ye H C, Huang W J, Qian B X, Wang J J, Lan Y B, et al. Inversion of maize leaf area index from UAV hyperspectral and multispectral imagery. Computers and Electronics in Agriculture, 2023; 212: 108020.

[48] Lu J S, Yang T C, Su X, Qi H, Yao X, Cheng T, et al. Monitoring leaf potassium content using hyperspectral vegetation indices in rice leaves. Precision Agriculture, 2020; 21: 324–348.

[49] Wen P F, Shi Z J, Li A, Ning F, Zhang Y H, Wang R, et al. Estimation of the vertically integrated leaf nitrogen content in maize using canopy hyperspectral red edge parameters. Precision Agriculture, 2021; 22: 984–1005.

[50] Guo J B, Zhang J J, Xiong S P, Zhang Z Y, Wei Q Q, Zhang W, et al. Hyperspectral assessment of leaf nitrogen accumulation for winter wheat using different regression modeling. Precision Agriculture, 2021; 22: 1634–1658.

[51] Patel M K, Ryu D, Western A W, Suter H, Young I M. Which multispectral indices robustly measure canopy nitrogen across seasons: Lessons from an irrigated pasture crop. Computers and Electronics in Agriculture, 2021; 182: 106000.

[52] Chen X K, Li F L, Shi B T, Chang Q R. Estimation of winter wheat plant nitrogen concentration from UAV hyperspectral remote sensing combined with machine learning methods. Remote Sensing, 2023; 15(11): 2831.

[53] Ta N, Chang Q R, Zhang Y M. Estimation of apple tree leaf chlorophyll content based on machine learning methods. Remote Sensing, 2021; 13(19): 3902.

[54] Fu Y Y, Yang G J, Li Z H, Li H L, Li Z H, Xu X G, et al. Progress of hyperspectral data processing and modelling for cereal crop nitrogen monitoring. Computers and Electronics in Agriculture, 2020; 172: 105321.

[55] Gahrouei O R, McNairn H, Hosseini M, Homayouni S. Estimation of crop biomass and leaf area index from multitemporal and multispectral imagery using machine learning approaches. Canadian Journal of Remote Sensing, 2020; 46(1): 84–99.

[56] Peng J X, Manevski K, Kørup K, Larsen R, Andersen M N. Random forest regression results in accurate assessment of potato nitrogen status based on multispectral data from different platforms and the critical concentration approach. Field Crops Research, 2021; 268: 108158.

[57] Zhang Y, Xia C Z, Zhang X Y, Cheng X H, Feng G Z, Wang Y, et al. Estimating the maize biomass by crop height and narrowband vegetation indices derived from UAV-based hyperspectral images. Ecological Indicators, 2021; 129: 107985.

[58] Ma L L, Chen X Y, Zhang Q, Lin J, Yin C X, Ma Y R, et al. Estimation of nitrogen content based on the hyperspectral vegetation indexes of interannual and multi-temporal in cotton. Agronomy, 2022; 12(6): 1319.

[59] Yang H B, Yin H, Li F, Hu Y C, Yu K. Machine learning models fed with optimized spectral indices to advance crop nitrogen monitoring. Field Crops Research, 2023; 293: 108844.

[60] Gao J, Shahid R, Ji X, Li S J. Climate change resilience and sustainable tropical agriculture: Farmers' perceptions, reactive adaptations and determinants of reactive adaptations in Hainan, China. Atmosphere, 2022; 13(6): 955.

[61] Hu N, Hu J C, Jiang X D, Xiao W, Yao K M, Li L, et al. Application of the maximum threshold distances to reduce gene flow frequency in the coexistence between genetically modified (GM) and non - GM maize. Evolutionary Applications, 2022; 15(3): 471–483.

[62] Xue L H, Cao W X, Luo W H, Dai T B, Zhu Y. Monitoring leaf nitrogen status in rice with canopy spectral reflectance. Agronomy Journal, 2004; 96(1): 135–142.

[63] Zarco-Tejada P J, Miller J R, Noland T L, Mohammed G H, Sampson P H. Scaling-up and model inversion methods with narrowband optical indices for chlorophyll content estimation in closed forest canopies with hyperspectral data. IEEE Transactions on Geoscience and Remote Sensing, 2001; 39(7): 1491–1507.

[64] Rouse J W. Monitoring the vernal advancement of retrogradation of natural vegetation. NASA/GSFC, TypeIII, Final report, Greenbelt, MD, 1974; pp.1–371.

[65] Jordan C F. Derivation of leaf area index from light quality of the forest floor. Ecology, 1969; 50(4): 663–666.

[66] Blackburn G A. Quantifying chlorophylls and caroteniods at leaf and canopy scales: An evaluation of some hyperspectral approaches. Remote Sensing of Environment, 1998; 66(3): 273–285.

[67] Gitelson A, Merzlyak M N. Quantitative estimation of chlorophyll-a using reflectance spectra: Experiments with autumn chestnut and maple leaves. Journal of Photochemistry and Photobiology B: Biology, 1994; 22(3): 247–252.

[68] Fitzgerald G J, Rodriguez D, Christensen L K, Belford R, Sadras V O, Clarke T R. Spectral and thermal sensing for nitrogen and water status in rainfed and irrigated wheat environments. Precision Agriculture, 2006; 7(4): 233–248.

[69] Jiang Z Y, Huete A R, Didan K, Miura T. Development of a two-band enhanced vegetation index without a blue band. Remote Sensing of Environment, 2008; 112(10): 3833–3845.

[70] Gitelson A A, Keydan G P, Merzlyak M N. Three-band model for noninvasive estimation of chlorophyll, carotenoids, and anthocyanin contents in higher plant leaves. Geophysical Research Letters, 2006; 33(11): 2006GL026457.

[71] Dash J, Curran P J. Evaluation of the MERIS terrestrial chlorophyll index (MTCI). Advances in Space Research, 2007; 39(1): 100–104.

[72] Castro K L, Sanchez-Azofeifa G A. Changes in spectral properties, chlorophyll content and internal mesophyll structure of senescing Populus balsamifera and Populus tremuloides leaves. Sensors, 2008; 8(1): 51–69.

[73] Rondeaux G, Steven M, Baret F. Optimization of soil-adjusted vegetation indices. Remote Sensing of Environment, 1996; 55(2): 95–107.

[74] Daughtry C S, Walthall C L, Kim M S, De Colstoun E B, McMurtrey Iii J E. Estimating corn leaf chlorophyll concentration from leaf and canopy reflectance. Remote Sensing of Environment, 2000; 74(2): 229–239.

[75] Gitelson A A, Kaufman Y J, Merzlyak M N. Use of a green channel in remote sensing of global vegetation from EOS-MODIS. Remote Sensing of Environment, 1996; 58(3): 289–298.

[76] Chen J M. Evaluation of vegetation indices and a modified simple ratio for boreal applications. Canadian Journal of Remote Sensing, 1996; 22(3): 229–242.

[77] Qi J, Chehbouni A, Huete A R, Kerr Y H, Sorooshian S. A modified soil adjusted vegetation index. Remote Sensing of Environment, 1994; 48(2): 119–126.

[78] Huete A R. A soil-adjusted vegetation index (SAVI). Remote Sensing of Environment, 1988; 25(3): 295–309.

[79] Lemaire G, Jeuffroy M H, Gastal F. Diagnosis tool for plant and crop N status in vegetative stage: Theory and practices for crop N management. European Journal of Agronomy, 2008; 28(4): 614–624.

[80] Li F, Mistele B, Hu Y C, Chen X P, Schmidhalter U. Comparing hyperspectral index optimization algorithms to estimate aerial N uptake using multi-temporal winter wheat datasets from contrasting climatic and geographic zones in China and Germany. Agricultural and Forest Meteorology, 2013; 180: 44–57.

[81] Feng W, Guo B B, Zhang H Y, He L, Zhang Y S, Wang Y H, et al. Remote estimation of above ground nitrogen uptake during vegetative growth in winter wheat using hyperspectral red-edge ratio data. Field Crops Research, 2015; 180: 197–206.

[82] Guyot G, Baret F, Major D. High spectral resolution: Determination of spectral shifts between the red and the near infrared. International Archives of Photogrammetry and Remote Sensing, 1988; 11: 750–760.

[83] Jin J, Pratama B A, Wang Q. Tracing leaf photosynthetic parameters using hyperspectral indices in an alpine deciduous forest. Remote Sensing, 2020; 12(7): 1124.

[84] Chen X Y, Lyu X, Ma L L, Chen A Q, Zhang Q, Zhang Z. Optimization and validation of hyperspectral estimation capability of cotton leaf nitrogen based on SPA and RF. Remote Sensing, 2022; 14(20): 5201.

[85] Song X, Xu D Y, Huang C C, Zhang K K, Huang S M, Guo D D, et al. Monitoring of nitrogen accumulation in wheat plants based on hyperspectral data. Remote Sensing Applications: Society and Environment, 2021; 23: 100598.

[86] Dong T F, Meng J H, Shang J L, Liu J G, Wu B F. Evaluation of chlorophyll-related vegetation indices using simulated Sentinel-2 data for estimation of crop fraction of absorbed photosynthetically active

radiation. IEEE Journal of Selected Topics in Applied Earth Observations and Remote Sensing, 2015; 8(8): 4049–4059.

[87] Nguy-Robertson A L, Gitelson A A. Algorithms for estimating green leaf area index in C3 and C4 crops for MODIS, Landsat TM/ETM+, MERIS, Sentinel MSI/OLCI, and Venμs sensors. Remote Sensing Letters, 2015; 6(5): 360–369.

[88] Li W, Li D, Liu S Y, Baret F, Ma Z Y, He C, et al. RSARE: A physically-based vegetation index for estimating wheat green LAI to mitigate the impact of leaf chlorophyll content and residue-soil background. ISPRS Journal of Photogrammetry and Remote Sensing, 2023; 200: 138–152.

[89] Ramos-García C A, Martínez-Martínez L J, Bernal-Riobo J H. Estimating chlorophyll and nitrogen contents in maize leaves (*Zea mays* L.) with spectroscopic analysis. Revista Colombiana de Ciencias Hortícolas, 2022; 16(1): 13398.

[90] Prey L, Von Bloh M, Schmidhalter U. Evaluating RGB imaging and multispectral active and hyperspectral passive sensing for assessing early plant vigor in winter wheat. Sensors, 2018; 18(9): 2931.

[91] Geipel J, Link J, Wirwahn J A, Claupein W. A programmable aerial multispectral camera system for in-season crop biomass and nitrogen content estimation. Agriculture, 2016; 6(1): 4.

[92] Verma B, Prasad R, Srivastava P K, Singh P. Retrieval of leaf area index using inversion algorithm. In: 2022 12th Workshop on Hyperspectral Imaging and Signal Processing: Evolution in Remote Sensing (WHISPERS), Rome: IEEE, 2022; pp.1–4.

[93] Fan X L, Lyu X, Gao P, Zhang L F, Zhang Z, Zhang Q, et al. Establishment of a monitoring model for the cotton leaf area index based on the canopy reflectance spectrum. Land, 2023; 12(1): 78.

[94] Tang Z J, Guo J J, Xiang Y Z, Lu X H, Wang Q, Wang H D, et al. Estimation of leaf area index and above-ground biomass of winter wheat based on optimal spectral index. Agronomy, 2022; 12(7): 1729.

[95] Liu S S, Bai X H, Zhu G G, Zhang Y, Li L T, Ren T, et al. Remote estimation of leaf nitrogen concentration in winter oilseed rape across growth stages and seasons by correcting for the canopy structural effect. Remote Sensing of Environment, 2023; 284: 113348.

[96] Liu J, Pattey E, Jégo G. Assessment of vegetation indices for regional crop green LAI estimation from Landsat images over multiple growing seasons. Remote Sensing of Environment, 2012; 123: 347–358.

[97] Guo F X, Feng Q, Yang S, Yang W X. Estimation of potato canopy nitrogen content based on hyperspectral index optimization. Agronomy, 2023; 13(7): 1693.

[98] Zhu Y, Li Y X, Feng W, Tian Y C, Yao X, Cao W X. Monitoring leaf nitrogen in wheat using canopy reflectance spectra. Canadian Journal of Plant Science, 2006; 86(4): 1037–1046.

[99] He L, Zhang H Y, Zhang Y S, Song X, Feng W, Kang G Z, et al. Estimating canopy leaf nitrogen concentration in winter wheat based on multi-angular hyperspectral remote sensing. European Journal of Agronomy, 2016; 73: 170–185.

[100] Inoue Y, Sakaiya E, Zhu Y, Takahashi W. Diagnostic mapping of canopy nitrogen content in rice based on hyperspectral measurements. Remote Sensing of Environment, 2012; 126: 210–221.

[101] Miphokasap P, Honda K, Vaiphasa C, Souris M, Nagai M. Estimating canopy nitrogen concentration in sugarcane using field imaging spectroscopy. Remote Sensing, 2012; 4(6): 1651–1670.

[102] Fu Y Y, Yang G J, Pu R L, Li Z H, Li H L, Xu X G, et al. An overview of crop nitrogen status assessment using hyperspectral remote sensing: Current status and perspectives. European Journal of Agronomy, 2021; 124: 126241.

[103] Cabrera-Bosquet L, Molero G, Stellacci A, Bort J, Nogués S, Araus J. NDVI as a potential tool for predicting biomass, plant nitrogen content and growth in wheat genotypes subjected to different water and nitrogen conditions. Cereal Research Communications, 2011; 39(1): 147–159.

[104] Yao X, Zhu Y, Tian Y C, Feng W, Cao W X. Exploring hyperspectral bands and estimation indices for leaf nitrogen accumulation in wheat. International Journal of Applied Earth Observation and Geoinformation, 2010; 12(2): 89–100.

[105] Song X, Xu D Y, He L, Feng W, Wang Y H, Wang Z J, et al. Using multi-angle hyperspectral data to monitor canopy leaf nitrogen content of wheat. Precision Agriculture, 2016; 17: 721–736.

[106] Alkhaled A, Townsend P A, Wang Y. Remote sensing for monitoring potato nitrogen status. American Journal of Potato Research, 2023; 100(1): 1–14.

[107] Ye H C, Huang W J, Huang S Y, Wu B, Dong Y Y, Cui B. Remote estimation of nitrogen vertical distribution by consideration of maize geometry characteristics. Remote Sensing, 2018; 10(12): 1995.

[108] Mallick J, AlMesfer M K, Singh V P, Falqi I I, Singh C K, Alsubih M, et al. Evaluating the NDVI-rainfall relationship in Bisha watershed, Saudi Arabia using non-stationary modeling technique. Atmosphere, 2021; 12(5): 593.

[109] Sims D A, Gamon J A. Relationships between leaf pigment content and spectral reflectance across a wide range of species, leaf structures and developmental stages. Remote Sensing of Environment, 2002; 81(2-3): 337–354.

[110] Li F L, Wang L, Liu J, Wang Y N, Chang Q R. Evaluation of leaf N concentration in winter wheat based on discrete wavelet transform analysis. Remote Sensing, 2019; 11(11): 1331.

[111] Wang X X, Cai G S, Lu X P, Yang Z N, Zhang X J, Zhang Q G. Inversion of wheat leaf area index by multivariate red-edge spectral vegetation index. Sustainability, 2022; 14(23): 15875.

[112] Yang H B, Li F, Hu Y C, Yu K. Hyperspectral indices optimization algorithms for estimating canopy nitrogen concentration in potato (*Solanum tuberosum* L.). International Journal of Applied Earth Observation and Geoinformation, 2021; 102: 102416.

[113] Guo B B, Zhu Y J, Feng W, He L, Wu Y P, Zhou Y, et al. Remotely estimating aerial N uptake in winter wheat using red-edge area index from multi-angular hyperspectral data. Frontiers in Plant Science, 2018; 9: 675–688.

[114] Fan K, Li F L, Chen X K, Li Z F, Mulla D J. Nitrogen balance index prediction of winter wheat by canopy hyperspectral transformation and machine learning. Remote Sensing, 2022; 14(14): 3504.

[115] Homolová L, Malenovský Z, Clevers J G, García-Santos G, Schaepman M E. Review of optical-based remote sensing for plant trait mapping. Ecological Complexity, 2013; 15: 1–16.

[116] Baret F, Houlès V, Guerif M. Quantification of plant stress using remote sensing observations and crop models: the case of nitrogen management. Journal of experimental botany, 2007; 58(4): 869–880.

[117] Cartelat A, Cerovic Z G, Goulas Y, Meyer S, Lelarge C, Prioul J L, et al. Optically assessed contents of leaf polyphenolics and chlorophyll as indicators of nitrogen deficiency in wheat (*Triticum aestivum* L.). Field crops research, 2005; 91(1): 35–49.

[118] Osco L P, Ramos A P M, Pereira D R, Moriya R A S, José Eduardo Creste. Predicting canopy nitrogen content in citrus-trees using random forest algorithm associated to spectral vegetation indices from UAV-imagery. Remote Sensing, 2019; 11(24): 2925.

[119] Osco L P, Junior J M, Ramos A P M, Furuya D E G, Santana D C, Teodoro L P R, et al. Leaf nitrogen concentration and plant height prediction for maize using UAV-based multispectral imagery and machine learning techniques. Remote Sensing, 2020; 12(19): 3237.

[120] Marang I J, Filipp.P, Weaver T B, Evans B J, Whelan B M, Bishop T F, et al. Machine learning optimised hyperspectral remote sensing retrieves cotton nitrogen status. Remote Sensing, 2021; 13(8): 1428.

[121] Zha H N, Miao Y X, Wang T T, Li Y, Zhang J, Sun W C, et al. Improving unmanned aerial vehicle remote sensing-based rice nitrogen nutrition index prediction with machine learning. Remote Sensing, 2020; 12(2): 215.

[122] Liu S Y, Zhang B, Yang W G, Chen T, Zhang H, Lin Y D, et al. Quantification of physiological parameters of rice varieties based on multi-spectral remote sensing and machine learning models. Remote Sensing, 2023; 15(2): 453.

[123] Johansen K, Morton M J L, Malbeteau Y, Aragon B, Al-Mashharawi S, Ziliani M G, et al. Predicting biomass and yield in a tomato phenotyping experiment using UAV imagery and random forest. Frontiers in Artificial Intelligence, 2020; 3: 28.

[124] Zhou K, Cheng T, Zhu Y, Cao W X, Ustin S L, Zheng H, et al. Assessing the impact of spatial resolution on the estimation of leaf nitrogen concentration over the full season of paddy rice using near-surface imaging spectroscopy data. Frontiers in Plant Science, 2018; 9: 964.

[125] Inoue Y, Darvishzadeh R, Skidmore A. Hyperspectral assessment of ecophysiological functioning for diagnostics of crops and vegetation. In: Thenkabail P S, Lyon J G, Huete A (Ed.), editors. Biophysical and biochemical characterization and plant species studies. CRC Press. 2018. pp.25–71.

[126] Wang L, Chang Q R, Li F L, Yan L, Huang Y, Wang Q, et al. Effects of growth stage development on paddy rice leaf area index prediction models. Remote Sensing, 2019; 11(3): 361.

[127] Chen X K, Li F L, Wang Y N, Shi B T, Hou Y H, Chang Q R. Estimation of winter wheat leaf area index based on UAV hyperspectral remote sensing. Transactions of the CSAE, 2020; 36(22): 40–49. (in Chinese)
[128] Breiman L. Random Forests. Machine Learning, 2001; 45: 5–32.
[129] Jiang J, Johansen K, Stanschewski C S, Wellman G, Mousa M A, Fiene G M, et al. Phenotyping a diversity panel of quinoa using UAV-retrieved leaf area index, SPAD-based chlorophyll and a random forest approach. Precision Agriculture, 2022; 23(3): 961–983.
[130] Han L, Yang G J, Dai H Y, Xu B, Yang H, Feng H K, et al. Modeling maize above-ground biomass based on machine learning approaches using UAV remote-sensing data. Plant Methods, 2019; 15(1): 10.
[131] Maxwell A E, Warner T A, Fang F. Implementation of machine-learning classification in remote sensing: An applied review. International Journal of Remote Sensing, 2018; 39(9): 2784–2817.
[132] Polikar R. Ensemble based systems in decision making. IEEE Circuits and Systems Magazine, 2006; 6(3): 21–45.
[133] Wang J J, Chen Y Y, Chen F F, Shi T Z, Wu G F. Wavelet-based coupling of leaf and canopy reflectance spectra to improve the estimation accuracy of foliar nitrogen concentration. Agricultural and Forest Meteorology, 2018; 248: 306–315.
[134] Shah S H, Angel Y, Houborg R, Ali S, McCabe M F. A random forest machine learning approach for the retrieval of leaf chlorophyll content in wheat. Remote Sensing, 2019; 11(8): 920.
[135] Qiu Z C, Ma F, Li Z W, Xu X B, Ge H X, Du C W. Estimation of nitrogen nutrition index in rice from UAV RGB images coupled with machine learning algorithms. Computers and Electronics in Agriculture, 2021; 189: 106421.
[136] Sun Q, Jiao Q, Qian X, Liu L, Liu X, Dai H. Improving the retrieval of crop canopy chlorophyll content using vegetation index combinations. Remote Sensing, 2021; 13(3): 470.
[137] Liang L, Di L P, Huang T, Wang J H, Lin L, Wang L J, et al. Estimation of leaf nitrogen content in wheat using new hyperspectral indices and a random forest regression algorithm. Remote Sensing, 2018; 10(12): 1940.
[138] Singh H, Roy A, Setia R K, Pateriya B. Estimation of nitrogen content in wheat from proximal hyperspectral data using machine learning and explainable artificial intelligence (XAI) approach. Modeling Earth Systems and Environment, 2022; 8: 2505–2511.
[139] Nigon T J, Yang C, Dias Paiao G, Mulla D J, Knight J F, Fernández F G. Prediction of early season nitrogen uptake in maize using high-resolution aerial hyperspectral imagery. Remote Sensing, 2020; 12(8): 1234.
[140] Guo B B, Qi S L, Heng Y R, Duan J Z, Zhang H Y, Wu Y P, et al. Remotely assessing leaf N uptake in winter wheat based on canopy hyperspectral red-edge absorption. European Journal of Agronomy, 2017; 82: 113–124.
[141] Li L T, Lu J W, Wang S Q, Ma Y, Wei Q Q, Li X K, et al. Methods for estimating leaf nitrogen concentration of winter oilseed rape (*Brassica napus* L.) using in situ leaf spectroscopy. Industrial Crops and Products, 2016; 91: 194–204.
[142] Ryu C, Suguri M, Iida M, Umeda M, Lee C. Integrating remote sensing and GIS for prediction of rice protein contents. Precision Agriculture, 2011; 12: 378–394.
[143] Wen P F, He J, Ning F, Wang R, Zhang Y H, Li J. Estimating leaf nitrogen concentration considering unsynchronized maize growth stages with canopy hyperspectral technique. Ecological Indicators, 2019; 107: 105590.
[144] Wang L, Chen S S, Li D, Wang C Y, Jiang H, Zheng Q, et al. Estimation of paddy rice nitrogen content and accumulation both at leaf and plant levels from UAV hyperspectral imagery. Remote Sensing, 2021; 13(15): 2956.
[145] Chen Q W, Mu X H, Chen F J, Yuan L X, Mi G H. Dynamic change of mineral nutrient content in different plant organs during the grain filling stage in maize grown under contrasting nitrogen supply. European Journal of Agronomy, 2016; 80: 137–153.
[146] Mu X, Chen Q, Chen F, Yuan L, Mi G. Dynamic remobilization of leaf nitrogen components in relation to photosynthetic rate during grain filling in maize. Plant Physiology and biochemistry, 2018; 129: 27–34.
[147] Lu J S, Cheng D L, Geng C M, Zhang Z T, Xiang Y Z, Hu T T. Combining plant height, canopy coverage and vegetation index from UAV-based RGB images to estimate leaf nitrogen concentration of summer maize. Biosystems Engineering, 2021; 202: 42–54.
[148] Du B M, Ji H W, Peng C, Liu X J, Liu C J. Altitudinal patterns of leaf stoichiometry and nutrient resorption in *Quercus variabilis* in the Baotianman Mountains, China. Plant and Soil, 2017; 413: 193–202.
[149] Huang Y T, Lu Y L, Ding Y, Yu Z B, Cheng H. Comparison of soil nutrient status in four types of forests in Bawangling of Hainan island. Journal of West China Forestry Science, 2013; 42(1): 64–69.
[150] Lin Y Q, Wang A W, Su P, Fu H S. Distribution characteristics of soil nutrients in the western region of Hainan - Taking Baisha Li Autonomous County as an Example. China Tropical Agriculture, 2017; 14(1): 32–35.
[151] Cambouris A N, Ziadi N, Perron I, Alotaibi K D, St. Luce M, Tremblay N. Corn yield components response to nitrogen fertilizer as a function of soil texture. Canadian Journal of Soil Science, 2016; 96(4): 386–399.
[152] Zhao C X, Jia L H, Wang Y F, Wang M L, McGiffen Jr M E. Effects of different soil texture on peanut growth and development. Communications in Soil Science and Plant Analysis, 2015; 46(18): 2249–2257.
[153] Jalota S K, Singh S, Chahal G B S, Ray S S, Panigraghy S, Singh K B. Soil texture, climate and management effects on plant growth, grain yield and water use by rainfed maize - wheat cropping system: Field and simulation study. Agricultural Water Management, 2010; 97(1): 83–90.
[154] Li R F, Liu P, Dong S T, Zhang J W, Zhao B. Increased maize plant population induced leaf senescence, suppressed root growth, nitrogen uptake, and grain yield. Agronomy Journal, 2019; 111(4): 1581–1591.
[155] Testa G, Reyneri A, Blandino M. Maize grain yield enhancement through high plant density cultivation with different inter-row and intra-row spacings. European Journal of Agronomy, 2016; 72: 28–37.